Engineering of Perovskite Composite Materials for Optoelectronic Applications

Mukhammadali Ibragim, Bachelor of Engineering

Submitted in fulfilment of the requirements for the degree of Master of Science in Electrical and Computer Engineering

School of Engineering and Digital Sciences

Department of Electrical and Computer Engineering

Nazarbayev University

53 Kabanbay Batyr Avenue,

Astana, Kazakhstan, 010000

Main Supervisor: Annie Ng

Co-supervisor: Mehdi Shafiee

April 2025

Abstract

The potential application of perovskite nanocrystals (PNCs) in future optoelectronic devices is growing rapidly because of their adjustable bandgap properties, narrow emission linewidths and their high photoluminescence quantum yield (PLQY). Their operational deployment faces severe limitations because they become unstable when subjected to environmental elements like moisture, oxygen, heat, and light. This thesis studies various polymer matrices such as PMMA, PDMS, and PMHS for encapsulating perovskite quantum dots (PQDs) to improve their environmental durability while preserving their optical properties. PMMA facilitated the production of stable films resistant to water while the creation of SiO_2-based core-shell structures provided enhanced protection that significantly increased stability during extended water exposure. PDMS provided superior processability and flexibility for downconversion and LED encapsulation applications but presented moderate intensity trade-offs. Despite its mechanical brittleness and optical quenching properties PMHS enabled the development of a PQD powder which expanded its application range. The comparative analysis of the polymers revealed their individual strengths and limitations which indicated that choosing the appropriate material depends on specific application requirements. PDMS and PMMA-based composite tactile sensors provided practical demonstrations where PQD markers enabled accurate force-sensitive tracking when activated by UV light. The performance of PQD-polymer composites demonstrated their wide-ranging capabilities. Research results demonstrate that merging polymer engineering with quantum dot surface modifications like core-shell techniques broadens the functional scope of perovskite nanomaterials.

Table of Contents

List of Figures

Chapter 1 - Introduction

Perovskite nanocrystals (PNCs) are propitious materials for future semiconducting devices and applications. Numerous benefits are common for them such as variable bandgap energy, robust defect tolerance, and remarkable optical properties which makes them desirable candidates for next generation of photovoltaics (PV) and light emitting devices(LED). Their ordinary structure consists of two metal cations and three halide anions forming ABX_3 chemical structures where A and B are metal cations, X is halide anions [1,2,3]. Besides PNCs perovskite thin films are common composite in semiconductor industry, too. In contrast with PNCs, thin films have considerable low PLQY due minimal thickness of material.

Hot injection is currently one of the most popular methods in the synthesis of inorganic perovskites. The synthesis at high temperatures enables the tuning of shape and phase of the material. Particles of different sizes can be obtained by variation in injection temperature between 120 and 170°C [1]. It is also possible to control the photoluminescence phase by changing the halide component. These materials, after synthesis, usually need to be purified by multi-step centrifugation; this process separates the main material from residual by-products.

Synthesized material valuable in many branches of electronics like light emitting diodes (LED), solar cells, display technologies and various sensors. LEDs employing metal halides represent colossal market opportunities, with formidable applications in display technology, medicine, and optical communication [2,3]. By changing the bandgap, one is able to change the color of luminescence in LED, thereby achieving bright light output at low voltage with reduced heat generation and an extended life span; thus, it reduces cost operations [4]. Besides, by alloying their composition, inorganic semiconductors can also be tuned to emit a wide spectrum from ultraviolet down to near-infrared. For instance using PQDs may increase the color sharpness of modern display technologies due to sharp full width half maxima (FWHM) and high photoluminescence quantum yield (PLQY) [5].

Despite the large number of advantages, their instability remains a big problem limiting the use of metal halide perovskites in industries [6]. PNCs are highly sensitive to environmental factors such as moisture, fluctuations in temperature, and even light [7]. The embedding of PNC

into a polymer matrix has recently been proposed as a promising solution for these kinds of problems. Thus far, a wide range of different polymers has been explored as composite-forming agents for PNCs and stand as potential solutions for stability problems at hand [8]. The advantages of using polymers in perovskites are due to their properties, which include insulation against moisture and oxygen, chemical resistance, transparency, and compatibility with perovskites [9].

Chapter 2 - Literature Review

Formation of perovskite nanocomposites involving polymer bonding has a variety of methods such as blending, shrinking and swelling, and electrospinning. These techniques have their advantages depending on the cost effectiveness and quality of the resulting material. Adding external components such as carbon nanostructure, metal nanowires and conductive polymers may enhance electrical properties of composite materials.

2.1 Polymer composites

In fact, previous works have already demonstrated that physical blending of polymers with PNCs normally improves the stability and physical properties. Materials tried so far are poly(methyl methacrylate) (PMMA), polystyrene (PS), poly(styrene-ethylene-butylene-styrene) (SEBS), and poly(lauryl methacrylate) (PLMA) [9], among many others. In many cases, perovskite composites were synthesized in the controlled evaporation method for the solvent[10]. This approach normally results, in many instances, in poor film formation characterized by size and thickness increase and modification in morphology when films are spin-coated. However, optimization of the spin-coating process has enhanced these issues, hence making physical blending a very easy and promising method for the manufacturing of materials based on perovskite[11].

Another important technique, a version of physical blending, is the "swelling-shrinking" method of forming nanocomposites. This method makes use of the property of the solubility of polymers when immersed into different environments where they would swell and expand or shrink depending on which solvent is used as a result of the thermodynamic principles involved [12]. The preparation of PNC/polymer nanocomposites consists of mixing a solvent compatible with the polymer and $CsPbBr_3$ PNCs; then addition of the less favorable solvent, such as hexane, pauses the shrinking of the polymer. The whole process makes it possible to control the loading density of $CsPbBr_3$ PNCs precisely, since the mass or volume ratio between the PNCs and polymer matrices is adjusted accordingly. Therefore, it is fast in fabricating PNC/polymer nanocomposites under ambient conditions without inert gas protection, thus overcoming several major phase separation challenges associated with spin-coating and controlled solvent drying

methods. Therefore, in such nanocomposites, $CsPbBr_3$ PNCs do not lose their photoluminescence under UV light irradiation.

The most accessible methods for microfiber production, electrospinning has also been utilized in the fabrication of PNC/polymer nanocomposites. Recently, $CsPbBr_3$ PNCs were utilized to develop electrospun microfibers from PMMA and poly(vinylpyrrolidone) (PVP), where advances in production could be achieved by tuning flow rates, applied voltage, and the distance between the needle and collector. The optical properties of $CsPbBr_3$ PNC particles fixed on a CuO-microsheet surface are well preserved after this process[13].

Moreover, in combination with the microfluidic system, electro-spinning enabled the mass production of $CsPbBr_3$/PMMA fiber nanocomposites at room temperature without toxic waste [14]. The resulting microfibers had stable color purity with suitable optical properties and hence are suited for mass production. This therefore points out that PNC-based nanocomposites can be ideal materials for large-scale applications.

Another method of preserving and enhancing optical properties of PNCs is embedding them in glass lattice [5]. Amorphous inorganic glass provides suitable environment for growth of $CsPbX_3$ structures inside of crystalline matrix which passivates chemical activity of particles [15] and compact arrangement of framework. Such technique prevents aggregation and phase shifts due to insulating properties of glass and is known as $CsPbX_3$@glass[16]. Besides improved stability and defect tolerance, crystalline matrices face issues related to reduced PLQY which can be solved by introducing polydimethylsiloxane (PDMS) powder. Such morphology approaches 100% PLQY for green $CsPbBr_3$ configuration and 80% for red $CsPbI_{1.5}Br_{1.5}$ configuration. Heat treatment crystallization and laser induced crystallization seems to be the most versatile technique with ability to control grain size of grown perovskites [17]. Both methods involve high temperature treatment which is costly for large scale productions and appears as a challenge. Replacing crystalline glass with polymer composite such as acrylic glass might resolve the issue of high temperature crystallization.

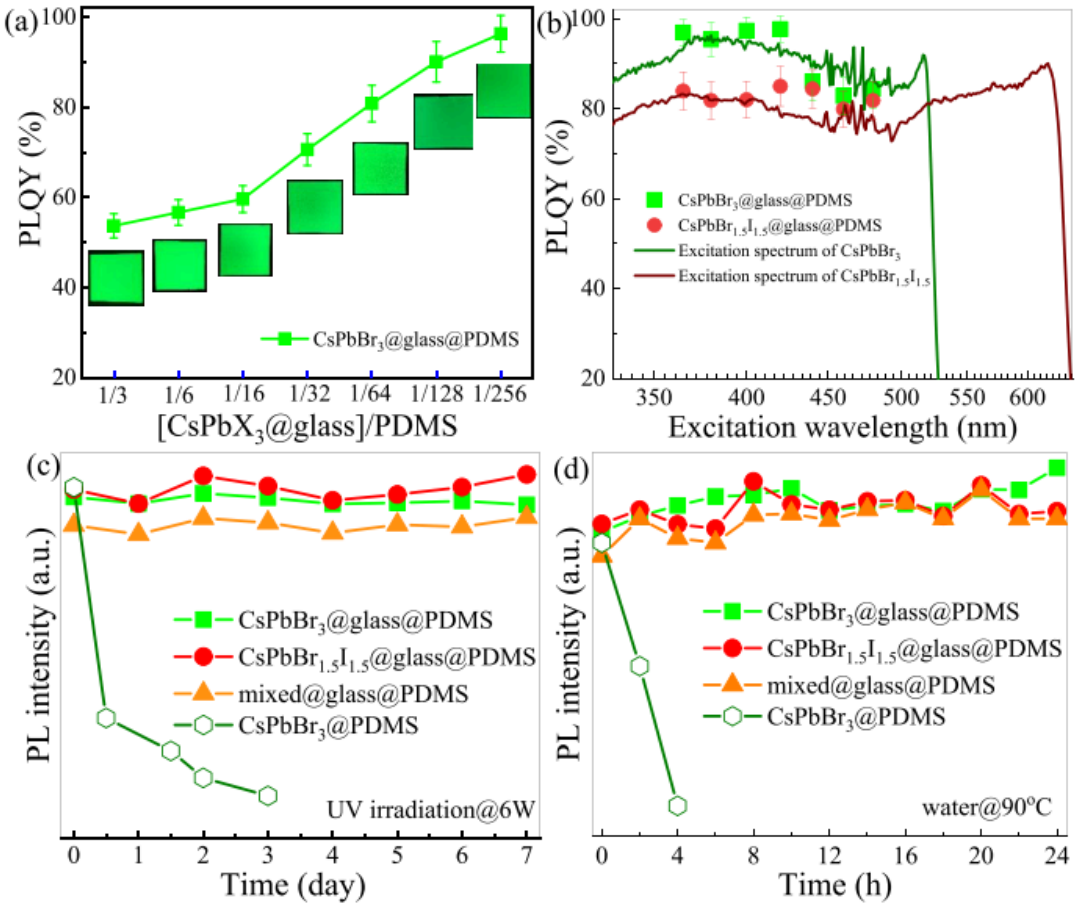

Figure 2.1. PLQY and PL stability graphs retrieved from [5]. a) PLQY dependence of $CsPbX_3$@glass : PDMS ratio, b) Light absorption of the material and it PLQY, c) Normalized PL stability for 7 days under UV irradiation for $CsPbX_3$ in different matrices, d) Normalized PL stability for 24 hours in water heated up to 90℃

2.2 Core-shell structures

Environmental factors including polar solvents, humidity and light exposure make Perovskite quantum dots (PQDs) unstable while they frequently show reduced photoluminescence quantum yield (PLQY). Researchers have focused significant attention on modifying LHPs to overcome these challenges and core-shell structures stand out as a particularly promising solution. The core-shell structures offer protective coatings which

improve PQDs by enhancing their stability and PLQY. Hou *et al.* [18] developed a novel technique to synthesize polymer-coated core-shell colloidal perovskite nanocrystals. The researchers achieved the formation of stable $CsPbBr_3$ nanocrystals in multidentate polymer micelles using their innovative "co-polymer templated synthesis" method to create core-shell structures. The process showed superior stability when used with polar solvents and in thin-film applications. The multidentate capping shell passivates the perovskite surface while significantly enhancing its photostability in polar solvents.

Qixuan Zhong *et al*. [19] managed to create $CsPbBr_3@SiO_2$ core-shell nanoparticles which have one $CsPbBr_3$ nanocrystal inside each shell. The core-shell nanoparticles preserved their structure for four weeks when exposed to air while uncoated $CsPbBr_3$ nanocrystals experienced degradation after only three days. $CsPbBr_3@SiO_2$ nanoparticles maintained green light emission for 40 minutes when exposed to water and ultrasonic conditions while uncoated $CsPbBr_3$ nanocrystals completely disintegrated in 16 minutes under UV light. Yipeng Huang *et al.* Researchers created dual-coated $MAPbBr_3$ ($MA = CH_3NH_3^+$) perovskite nanocrystals which incorporated a functionalized SiO_2 layer with PVDF shell. The coating maintained excellent stability for more than one month in humid environments and during exposure to UV light. The shell's hydrophobic properties provided better stability while allowing the nanocrystals to remain afloat on water surfaces. $MAPbBr_3@SiO_2$/PVDF nanoparticles displayed high luminous efficiency of 147.5 lm/W when used as a green light emitter and managed to reach 120% of the National Television System Committee's color gamut.

Bo Qiao *et al.* [20] applied the traditional hot injection approach to produce $CsPbBr_3$ nanocrystals before altering their stoichiometry to obtain $CsPbBr_3/CsPb_2Br_5$ core-shell nanocrystals with an inactive 2D CsPb2Br5 shell layer. Exposure to ethanol resulted in neat $CsPbBr_3$ decomposition within five seconds while core-shell nanocrystals maintained their green photoluminescence. The core-shell nanocrystals displayed consistent photoluminescence when applied to ITO glass substrates through extended water contact but the neat $CsPbBr_3$ PQDs showed complete PL intensity loss after five days. The 2D $CsPb_2Br_5$ shell provides enhanced stability because it exhibits an indirect bandgap and lacks light emission which together create a

quantum well structure and hydrophobic surface. The $CsPbBr_3/CsPb_2Br_5$ core-shell nanocrystals demonstrate features that make them ideal for use in optoelectronic devices.

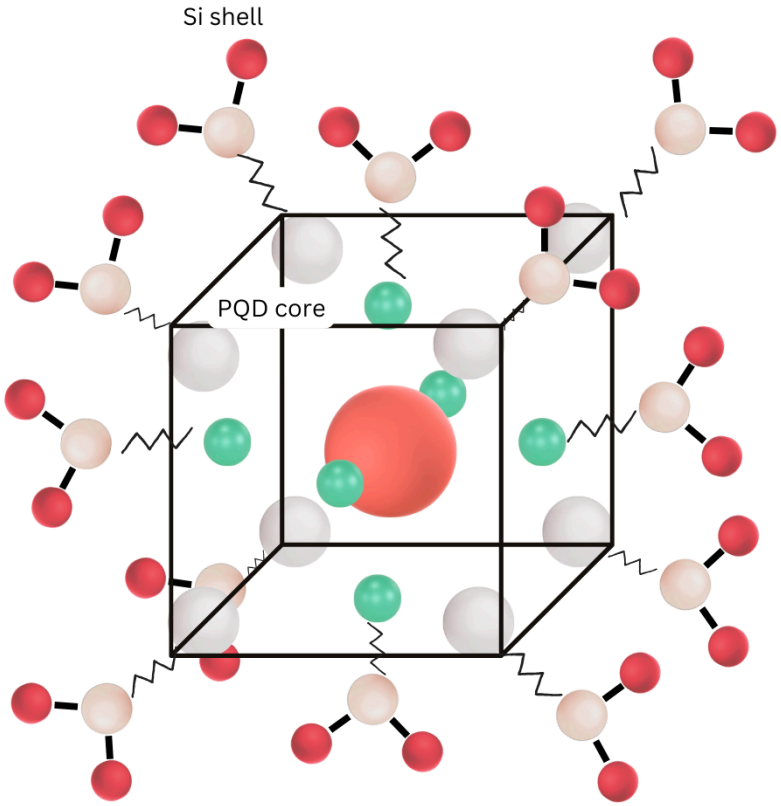

Figure 2.2. Schematic representation of cubic structure of core shell structure

2.3 LED applications

Huang *et al.* [21] produced $MAPbBr_3@SiO_2/PVDF$ nanoparticles through a process that involved soaking $MAPbBr_3$ solution into siliceous nanospheres for LED applications. The SiO_2 and PVDF shells served as a hydrophobic barrier that greatly improved the nanoparticles'

durability under water exposure and UV light. The photoluminescence range of these golden-green light emitters spanned 530–535 nm which made them suitable bright green light sources for LED applications. The $MAPbBr_3@SiO_2$/PVDF nanoparticles with core-shell structure showed success in meeting application requirements.

In their study Yuan *et al.* [22] created a consistent self-assembled core-shell structured flat $CsPbBr_3$ (SCQDs) film measuring 4.5 nm through a single-step precursor coating method suitable for flexible LED applications. Under ideal operating conditions green perovskite LEDs demonstrated an external quantum efficiency greater than 15%. The flexible device preserved 90% operational efficiency throughout 50 bending cycles that had a curvature radius of 1 cm. The potential use of luminescent solar concentrators spans exterior energy-efficient wall glass and flexible smart devices.

Figure 2.3. Photos of flexible LED based on SCQDs [22]

Figure 2.4. PQDs and PMMA based passive display for labeling exit sign under different illumination conditions : (i) 1200 lx, (ii) 600 lx, (iii) 300 lx, (iv) 300 lx under and UV excitation, and (v) 1 lx under and UV excitation [22]

The $CsPbX_3$@glass@PDMS backlight demonstrated successful functionality in LCD screens by providing a substantially wider color gamut. The $CsPbX_3$@glass LCD demonstrated superior color representation and increased saturation when compared to screens with commercial backlights. The PDMS matrix elasticity makes $CsPbX_3$@glass@PDMS films and designed backlit units viable for developing flexible displays.

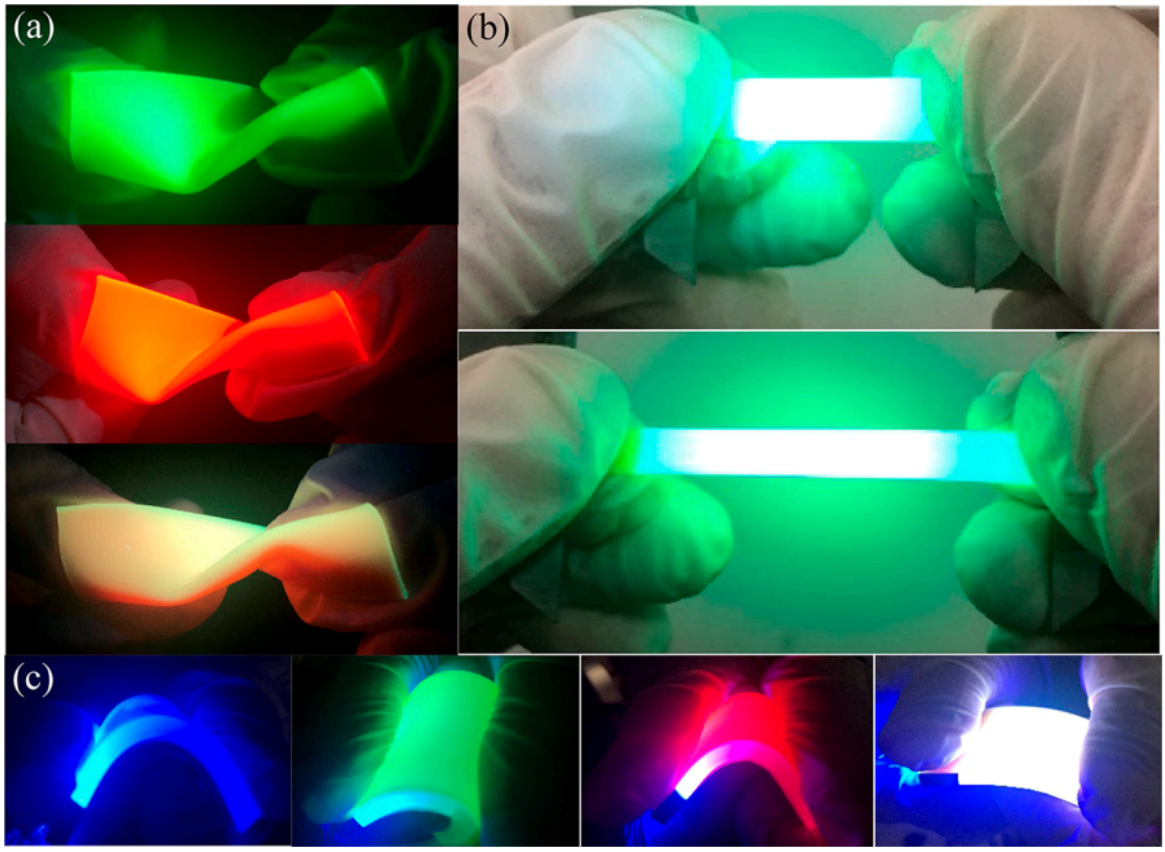

Figure 2.5. a) Luminescent images showcasing twisted $CsPbX_3$@glass@PDMS films in green, red, and yellow. b) Luminescent images of stretched green $CsPbBr_3$@glass@PDMS film. c) Flexible backlit units emitting blue, green, red, and white light for backlit LCD displays [22]

2.4 Tactile sensors

Sensors intended for input force measurement usually operate through capacitive, resistive, piezoelectric, or optical methods. Optical tactile sensors may utilize the photoluminescent properties of perovskite quantum dots for enhanced performance. Fiber Bragg Grating (FBG)-based optical tactile sensors are becoming increasingly popular because of their distinctive benefits. The structure of these sensors draws on human skin nerve fibers that convert mechanical movements into electrical signals and incorporates an optical fiber attached to an object. A light source with broad spectral output enters one end of the fiber while the detector on

the same end measures specific narrow-band wavelengths that are reflected. The difference between observed wavelengths (ΔλB) and the standard Bragg wavelength (λB) reveals both localized strain (Δε) and temperature changes (ΔT) according to the following formula [23]:

$$\frac{\Delta\lambda B}{\lambda B} = \{k_{\varepsilon}\Delta\varepsilon\} + \{k_{T}\Delta T\}$$

Here k_{ε} represents strain sensitivity while k_{T} stands for temperature sensitivity in this context. Because both strain and temperature affect the wavelength shift a second unstressed reference fiber is used to separate thermal influences. A number of FBG tactile sensors skip using multiple fibers which leads to potential measurement errors when operating in environments with variable conditions. New developments in tactile sensors that use optical fiber technology show promising applications across fields such as robotics and medical diagnostics. The AI-driven SOFT sensor represents a significant advancement by measuring 8 × 8 mm² and detecting contact points on a 2 × 3 array with 92.41% accuracy and an error rate below 4.2%. This sensor incorporates a stretchable three-layer laminate structure that extends beyond 20% with four integrated FBGs and functions in a force range from 0 to 3.5 N [24]. The sensor design depends on an oversized FBG integrator yet lacks temperature compensation which stands as a typical obstacle in FBG-based sensing technology. Additionally, testing was limited to single-contact scenarios .

A study [25] introduced a specklegram-based optical force sensor with a 20 mm diameter that measures 23 N strain using configurations of few-mode fiber (FMF) and multimode fiber (MMF). While the sensor detected strain intensity (sensitivity: The sensor detected strain intensity with a sensitivity of <0.087 N^{-1} and a standard deviation of 0.0219 yet failed to localize strain measurements and did not undergo any formal accuracy testing.

The nursing robot industry saw advancements with the introduction of a 3D-printed FBG tactile sensor [26]. The sensor system with four units positioned at a distance of 4 mm from one another delivered an exceptional sensitivity level of 225.038/N along with a quick response time of 2 ms and a 32.93 dB SNR while keeping error rates under 4.4%. This sensor demonstrated the ability to differentiate male and female pulse waveforms before and after physical activity. The

modular FBG-based tactile sensor research showed a sensitivity of 1.45 N and a spatial resolution of 1.91 mm and proved FBGs effective for RMIS because of their biocompatibility and resistance to corrosion which resistive and capacitive sensors lack.

For endoscopic applications researchers designed a six-axis FBG-based tactile sensor with temperature compensation which surpassed piezoelectric [27] sensors limited to single-axis force detection and capacitive [28] sensors which are non-biocompatible and MRI-incompatible. The system used a BPNN-based decoupling algorithm to identify FBG fractures and demonstrated its effectiveness during tests on phantom blood vessels with dimensions of 180 × 100 mm². Patient massage applications used a nursing-specific FBG sensor which incorporated four sensing elements formed through 3D printing with resin.

High costs and limited spatial resolution remain the main obstacles preventing FBG-based tactile sensors from achieving commercial availability despite technological progress. The exceptional properties of these sensors which include biocompatibility, electromagnetic immunity and distributed sensing make them an attractive solution for specialized medical applications such as robotics surgery and minimally invasive procedures.

Chapter 3 - Methodology

3.1 Perovskite Quantum Dots synthesis

The hot injection method enabled the synthesis of perovskite quantum dots (PQDs) with precision control over precursor preparation and reaction conditions. Before starting synthesis lead halide precursor amounts were measured precisely to match the target PQD composition. The preparation of $CsPbI_2Br$ involved using 0.101 grams of $PbBr_2$ and 0.311 grams of PbI_2 whereas $CsPbBr_3$ was prepared with 0.407 grams of $PbBr_2$ alone. The appropriate lead halide mixture dissolved in a three-neck flask contained 25 mL of octadecene to initiate the reaction. To achieve full dissolution and eliminate residual moisture the solution underwent vacuum treatment at 120°C in a sand bath for thirty minutes. The Cs-oleate preparation was kept at 80°C separately to preserve its optimal state for future injection steps. Two and a half milliliters of oleic acid and oleylamine were added to the lead halide solution to function as capping ligands after the initial heating phase. During the subsequent 30-minute heating phase the solution adopted an amber color which demonstrated successful precursor formation. The essential hot injection step took place at precisely controlled temperatures between 150°C and 200°C because higher temperatures resulted in bigger quantum dots through faster growth kinetics. During the injection process 2 mL of the preheated Cs-oleate solution is introduced into the reaction flask while maintaining continuous nitrogen flow. The rapid injection of the preheated Cs-oleate solution into the reaction flask under nitrogen flow initiated immediate nucleation and growth of PQDs which showed a brown color change in iodide systems and a bright lime green appearance in pure bromide systems. The reaction vessel underwent rapid cooling using an ice bath until it reached room temperature to halt particle growth and stabilize the colloidal solution. Centrifugation is used during the final purification stage to separate the quantum dots from reaction byproducts and leftover organic ligands. The production of monodisperse PQDs with precise optical properties was achieved through precise elimination of unreacted precursors and ligand aggregates. To obtain consistent photoluminescence characteristics each stage of the synthesis required both precise temperature management and accurate timing.

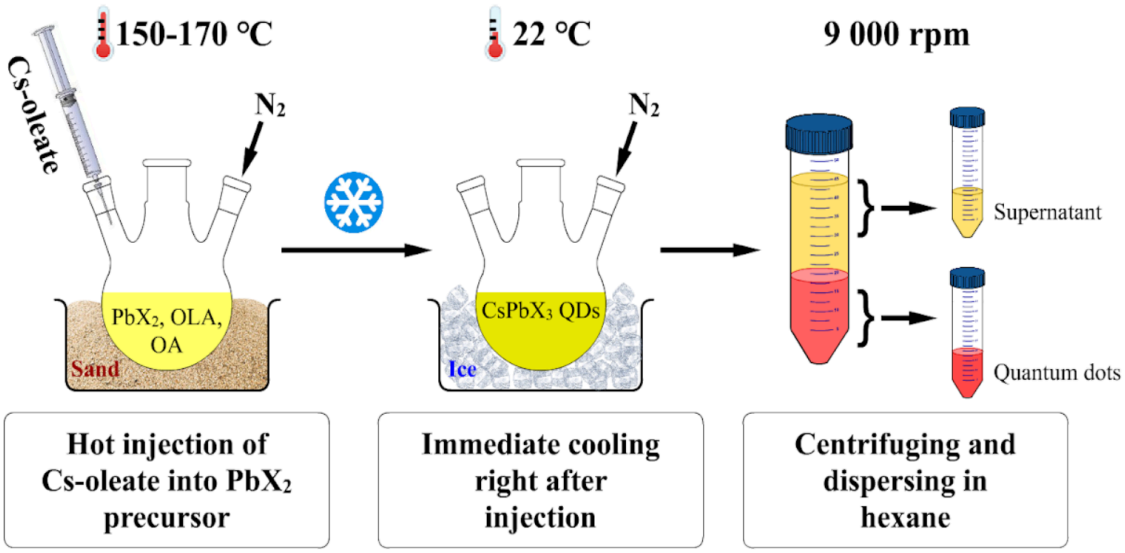

Figure 3.1. Schematic representation of PQD hot injection synthesis method used for preparation of luminescent particles

3.2 Preparation of PMMA films

Poly(methyl methacrylate) (PMMA) served as the matrix material for fabricating polymer composite films with perovskite quantum dots (PQDs). The process started by mixing 200 mg of PMMA powder with 1 mL of chlorobenzene (CB) in a hot plate set to 50°C while continuously stirring until a clear homogeneous solution formed. The polymer matrix received integration from either basic PQDs or core-shell structured PQDs during the PQD incorporation process. During the incorporation process the heated PMMA solution received a 400 µL quantum dot hexane suspension which was introduced dropwise while stirring remained constant. The process of adding nanocrystals to the polymer was meticulously controlled to distribute them evenly throughout the polymer matrix. The reaction proceeded under continuous stirring until the mixture showed a uniform green color which confirmed the homogeneous distribution of the luminescent PQDs. After thorough mixing the PQD-PMMA solution was transferred into a plastic mold where it gradually cooled to room temperature to form a solid transparent composite film. Gradual cooling enabled uniform solidification of the composite

material and blocked any phase separation or aggregation among the quantum dots. The production process relied on continuous stirring to achieve optimal PQD dispersion and consistent optical and mechanical properties in the resulting films. The composite films produced strong photoluminescence and preserved the structural integrity of the polymer matrix.

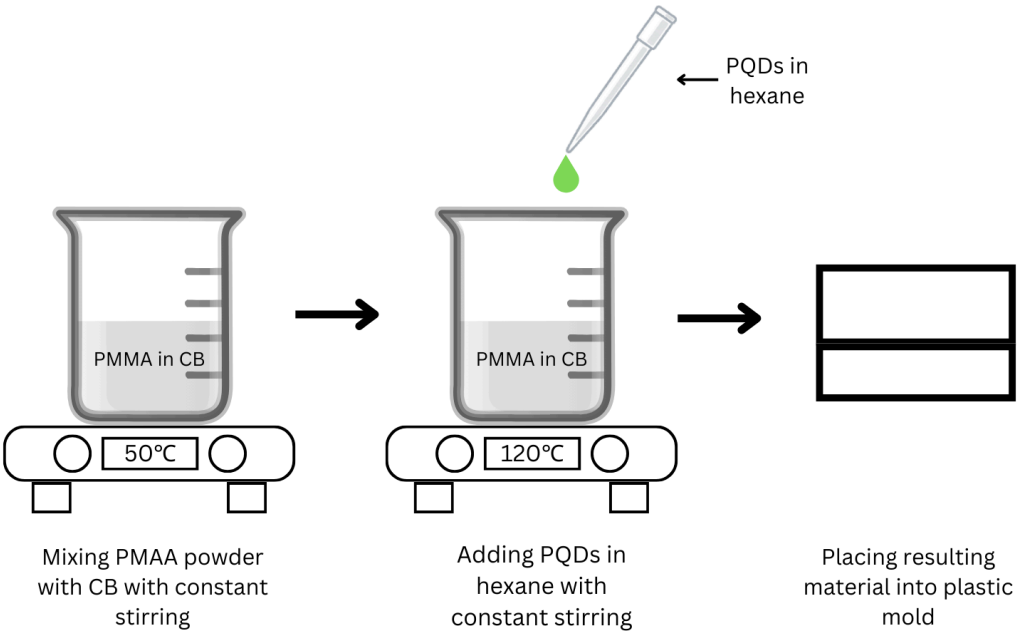

Figure 3.2. Schematic representation of the PMMA film preparation process

3.3 Core-shell structure preparation

For surface modification studies, 400 µL of perovskite quantum dot (PQD) solution in hexane (concentration: Researchers mixed a solution of perovskite quantum dots at 8.6 mg/mL with trimethoxy octyl silane in a 4 mL glass vial. The reaction mixture experienced continual stirring at 150 rpm while the experimental treatment duration varied systematically to study time-based effects under different conditions. The PQD samples treated with silane received

extensive characterization to study the effects of their surface functionalization. The treated quantum dots underwent photoluminescence spectroscopy tests to determine variations in their optical attributes as well as quantum yield. Transmission electron microscopy (TEM) used for study of the morphological adjustments and particle size distribution as well as potential aggregation behavior that occurred due to silane modification. By using this analytical method, we could establish connections between chemical treatment parameters and the consequent changes in luminescent performance together with nanoscale structural transformations of the PQDs.

3.4 Preparation of PDMS compound

A two-part poly(dimethyl siloxane) (PDMS) system (Sylgard-184) served as the base for preparing luminescent polymer composites. Achieving proper cross-linking of the elastomeric matrix required a weight ratio of 1:10 between base and curing agent. The homogenized PDMS mixture received a controlled dropwise addition of hexane-dispersed PQDs solution during mechanical stirring. It was precisely regulated the integration of the PQD solution to ensure nanocrystals spread evenly throughout the thick PDMS medium. After ensuring that the mixture had achieved homogeneous distribution through visual inspection, it was poured into its designated mold for the curing process. The composite material was allowed to cure under two alternative conditions: The composite can be cured either by allowing polymerization to progress slowly at room temperature over 24-48 hours or by speeding up cross-linking with a 2-hour exposure to 80°C.The fabrication method developed flexible PDMS films that were optically active with evenly distributed PQDs while preserving both the silicone matrix's elastomeric properties and the quantum dots' luminescent features. Application requirements determine the choice of curing protocol since room temperature curing produces more consistent dispersions whereas thermal curing results in quicker processing times. The created composites maintained stable photoluminescence properties alongside the natural mechanical flexibility of PDMS elastomers.

3.5 Preparation of PMHS film

PQD-embedded polymer composites were created by utilizing a thermal curing process. A precise measurement of azobisisobutyronitrile (AIBN) was taken to reach a concentration of 100 mg in each 1 mL portion of the poly(methylhydrosiloxane) (PMHS) matrix. The PMHS precursor received ultrasonic treatment alongside AIBN initiator powder for 15 minutes to dissolve the initiator completely and distribute it evenly throughout the siloxane polymer. The homogeneous precursor solution was carefully poured into a silicone mold which was chosen because of its non-stick properties to ensure easy removal of the cured polymer structure. During this step optimal dispersion of quantum dots in the polymer matrix was achieved by controlled dropwise introduction of hexane-dispersed PQDs while continuous mixing was maintained. The resulting mixture underwent complete homogenization until it displayed a uniform distribution of luminescent nanocrystals. The curing process was completed on a temperature-controlled hot plate set between 80-90°C which operated for 3 hours. During thermal exposure the PMHS matrix began radical polymerization while the residual hexane solvent evaporated. Elevated temperature curing enabled correct cross-linking of the polymer network and successful encapsulation of the PQDs which resulted in the formation of a strong nanocomposite material that maintained the optoelectronic characteristics of the embedded quantum dots in the transparent siloxane matrix.

3.6 Assembly of Tactile sensor

A custom-designed ABS plastic mold created through computer-aided design (CAD) and 3D printing produced the sensor assembly. The sensor's background layer involved casting black-colored silicone into the mold then pre-patterned with holes positioned precisely to fit luminescent markers. Perovskite quantum dots (PQDs) embedded into a poly(methyl methacrylate) (PMMA) matrix to create the markers. PQD-PMMA composite material uniformly mixed and then cast into a specialized silicone mold which shapes small round marker particles. The markers cured before carefully extracting them and placing them into the pre-designed holes in the black silicone background to ensure precise alignment which generated the detection

pattern. The sensor assembly received a soft silicone layer encapsulation after all markers achieved their proper positions and this silicone layer underwent curing to establish mechanical stability along with environmental protection. A thin layer of silicone coating was applied across the full sensor surface to boost durability while preserving optical clarity for effective quantum dot emission. A robust optical sensor was created through this multi-step fabrication process which included precisely arranged luminescent markers that enabled spatially resolved detection signals.

Chapter 4 - Results and Discussion

4.1 PQDs with PMMA

Perovskite quantum dot-polymer composite research showed outstanding humidity resistance as QDs@PMMA and QDs@SiO_2@PMMA films preserved their photoluminescence properties during 17 days of uninterrupted water exposure. The QDs@PMMA composite achieved enhanced moisture protection when hexane-suspended PQDs were dispersed within poly(methyl methacrylate) compared to standard quantum dot films without protection. The QDs@SiO_2@PMMA system achieved superior protection against hydrolytic degradation through the incorporation of a siloxane shell around PQDs. Throughout the test phases, the samples underwent regular removal from the immersion environment followed by compressed air drying to eliminate surface moisture before photoluminescence stability analysis. The core-shell structure proved to be highly beneficial for use cases that demand extended moisture exposure which represents a significant breakthrough in stabilizing perovskite quantum dots for real-world optoelectronic applications.

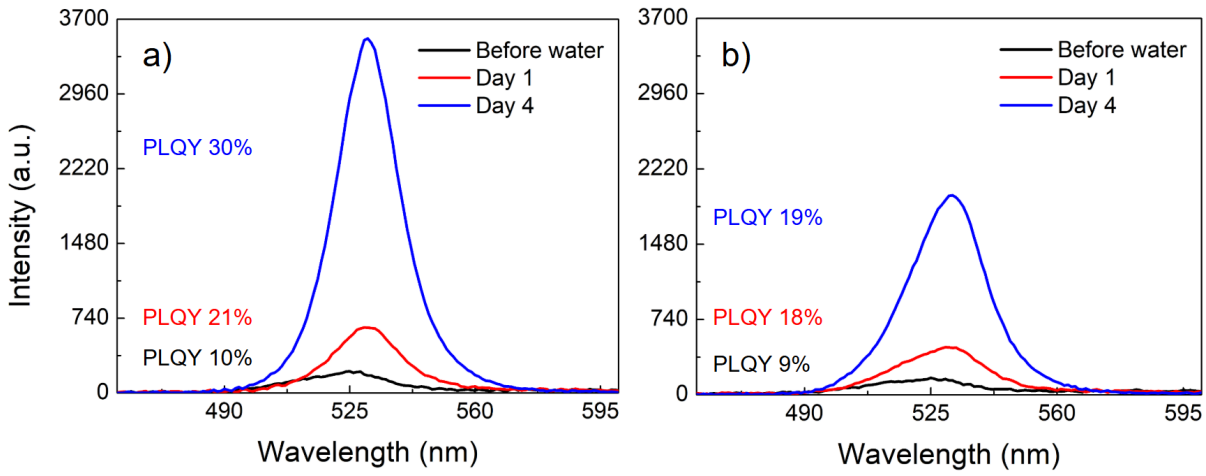

Figure 4.1. PL emission of the QDs@PMMA (a) and QDs@SiO_2@PMMA (b) films

Throughout the first 4-day exposure period both QDs@PMMA and QDs@SiO_2@PMMA samples showed increased photoluminescence (PL) emission intensity despite having different amplitude levels. The PMMA material's hygroscopic nature causes it to absorb water molecules from the surrounding environment over time. Reference [10] shows that water absorption by the PMMA matrix changes its optical behavior by allowing deeper light penetration and increased scattering in the polymer network which results in the observed PL enhancement effect. The PL intensity of core-shell QDs@SiO_2@PMMA composite consistently measured lower than that of its uncoated counterpart. This reduction stems from multiple factors: The siloxane shell surrounding the quantum dots exhibits inherent light-blocking properties that partially reduce both excitation and emission light while trimethoxy octyl silane (TMOS) functionalization boosts hydrophobicity. The octyl chains from TMOS establish a hydrophobic shield at the quantum dot-polymer interface which substantially reduces water absorption in the PMMA matrix of the core-shell composite as seen in Figure 4.1. PMMA's ability to enhance light penetration through water absorption competes with the light-attenuating moisture barrier function of the siloxane shell which leads to observable differences in photoluminescence behavior between both materials. Optoelectronic performance in PQD-polymer composites under humid conditions depends on the complex interactions between polymer matrix properties and quantum dot surface chemistry in addition to environmental factors.

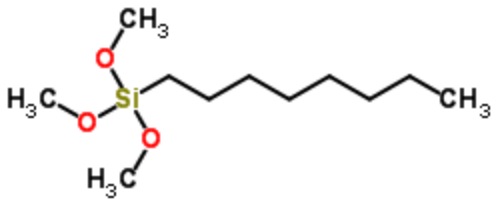

Figure 4.2. Chemical formula of TMOS

The creation of siloxane coatings on perovskite quantum dots through TMOS hydrolysis results in improved environmental stability but reduces optical performance. During core-shell preparation, the impact of stirring duration becomes more apparent because extended stirring time enables thicker siloxane shell formation (Figure 4.2). The examination of core-shell structures prior to polymer encapsulation reveals a definitive inverse correlation between stirring duration and photoluminescence intensity as shown in Figure 4.3. Prolonged reaction times enable full TMOS hydrolysis and condensation that produces denser siloxane coatings which reduce light transmission. The PL reduction stems from several concurrent factors: The reduction in photoluminescence originates from light scattering through the siloxane matrix as well as interfacial strain at the perovskite-siloxane boundary and modified exciton behaviors because of the dielectric shell. The main engineering challenge identified in core-shell PQD design involves striking a balance between ensuring adequate shell thickness for environmental protection and maintaining thin enough shells to sustain optimal light emission. Analysis indicates that there is an ideal processing range which maintains balance between these conflicting requirements for real-world device usage.

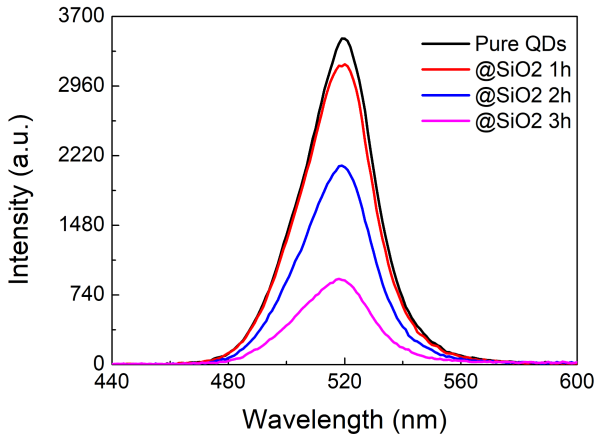

Figure 4.3. PL measurements of core-shell structure in comparison with pure PQDs and different stirring time with TMOS

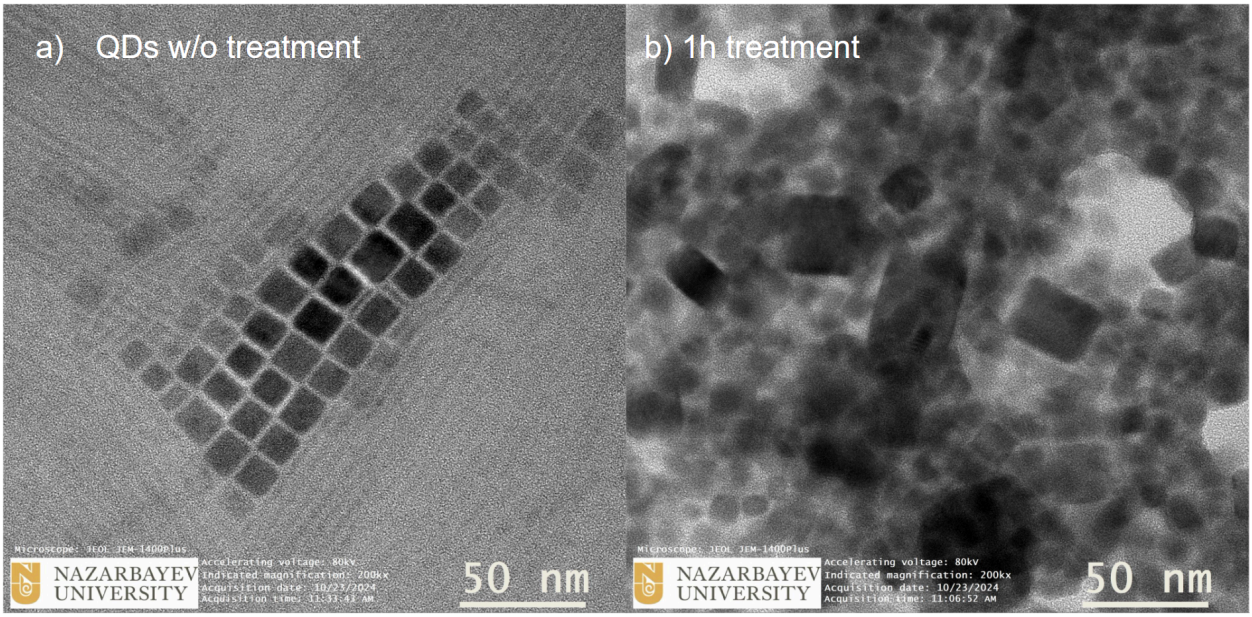

Figure 4.4 TEM images of PQDs before and after treatment with TMOS. a) Clean PQDs without treatment, b) PQDs after 1h treatment with TMOS

Figure 4.4 displays TEM results that firmly demonstrate the emergence of siloxane shells enveloping the perovskite quantum dots. Morphological disparities between untreated and TMOS-treated samples demonstrate core-shell nanostructure development. Untreated PQDs manifest as distinct crystalline particles which display sharp edges alongside uniform electron density that reflects high-quality perovskite nanocrystals. TMOS-treated samples show distinct shadow features around core particles which confirm successful siloxane layer deposition. The shadow regions demonstrate different thickness levels and conformal coatings that match the anticipated core-shell structure around the PQD cores. Transmission electron microscopy observations confirm the structural basis of the light-blocking mechanism for the siloxane shells. The photoluminescence quenching results from optical tests match the electron density changes observed at particle interfaces. The structural observations establish the basis for the notion that the siloxane shell physically blocks light emission which accounts for the observed consistent decrease in photoluminescence intensity as shell thickness grows. TEM images and optical

measurements together deliver complete verification of the core-shell formation process and its effects on quantum dot performance.

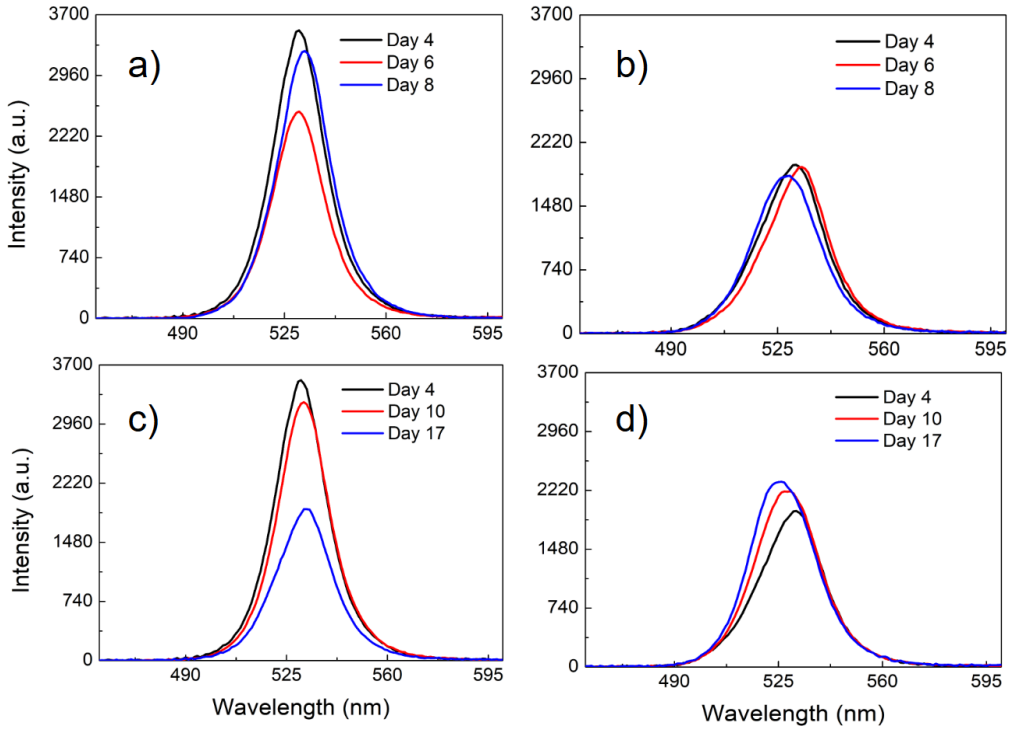

Figure 4.5. Extended PL emission measurements for samples at figure 4.1 from day 4 in water until day 17. QDs@PMMA (on the left) and QDs@SiO_2@PMMA (on the right) immersed in water.

Water immersion tests show siloxane-incorporated composites outperform pure PMMA-encapsulated quantum dots in stabilization. The QDs@SiO_2@PMMA system displays enhanced stability through minimal photoluminescence peak shifts during long-term water exposure which shows improved retention of the quantum dots' optical properties. The enhanced performance of the composite material results from two combined effects of the siloxane

component. The siloxane shell creates a physical barrier that prevents water from coming into contact with the perovskite core. The TMOS treatment is crucial because it incorporates hydrophobic octyl chains which notably enhance the material's resistance to water. The contact angle measurements demonstrate a significant improvement in hydrophobic properties of siloxane-containing composite compared to plain PMMA. The stability differences observed result from a dual protection mechanism where PMMA provides encapsulation benefits but its natural hygroscopic nature lets water slowly penetrate. The siloxane-modified system merges PMMA matrix protection with the superior moisture resistance provided by the organosilane components. Research shows a direct relationship between contact angles and photoluminescence stability which demonstrates that surface hydrophobization through siloxane functionalization offers effective protection against water-induced degradation of quantum dots. The findings emphasize that interfacial engineering plays a critical role in perovskite quantum dot composites because precise surface chemistry management greatly boosts material stability for use in moist or wet conditions. The siloxane-enhanced system shows that combining organic and inorganic components helps to surpass the constraints found in pure polymer encapsulation methods.

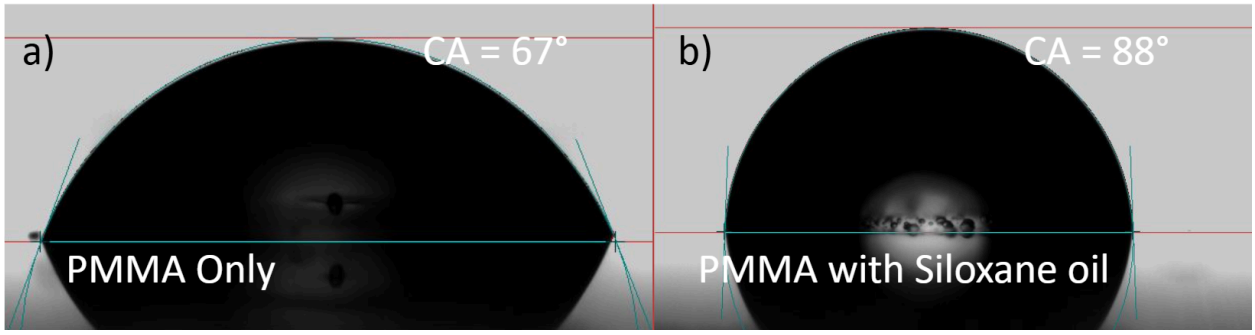

Figure 4.6. Monochromatic photo of contact angle measurement of PMMA film with (a) and without (b) additive Siloxane oil

Comprehensive analysis verifies that siloxane-containing composites exhibit superior stability according to theoretical predictions despite both encapsulation systems achieving significant moisture resistance. The photoluminescence tracking results from water-immersed samples demonstrate fundamentally different behavior patterns in these two material systems. Throughout the testing period the QDs@PMMA control sample demonstrates significant instability as its peak intensity fluctuates between 1850 and 3500 arbitrary units without a consistent pattern. The observed fluctuations reveal continuous water infiltration and interface breakdown without siloxane protection. After an initial 4-day adjustment period the QDs@SiO_2@PMMA composite demonstrates exceptional stability which maintains uniform emission intensity throughout day 8 with minor PL enhancement reaching about 2400 a.u. This performance differential originates from multiple stabilizing factors in the core-shell system: Surface groups that come from TMOS form a moisture barrier due to their hydrophobic properties and the siloxane interlayer serves as a physical shield protecting the perovskite core from water exposure. The modified polymer interface within the siloxane-containing composite functions to minimize harmful interactions between water and the matrix.. Hybrid organic-inorganic stabilization approaches show effectiveness in solving the environmental sensitivity problems of perovskite quantum dots for real-world uses.

4.2 PQDs with PDMS

The unique chemical and physical properties of poly(dimethyl siloxane) (PDMS) make it an effective matrix for encapsulating perovskite quantum dots. The two-component system combines a PDMS polymer with a curing agent which upon mixing triggers cross-linking reactions to produce a solid elastomer. The curing process allows processing at both room temperature to protect sensitive PQDs from thermal damage and higher temperatures for quicker

solidification. Uncured PDMS displays outstanding moldability which enables the production of PQD-embedded composites across multiple geometries including optical-grade thin films and specific three-dimensional structures. Such versatility is related to working as a liquid before curing while maintaining accurate shape replication once it solidifies. PDMS delivers strong environmental protection to encapsulated quantum dots by utilizing several protective mechanisms. PDMS forms an effective moisture barrier because of its hydrophobic properties while its tightly cross-linked network structure restricts oxygen diffusion [29].

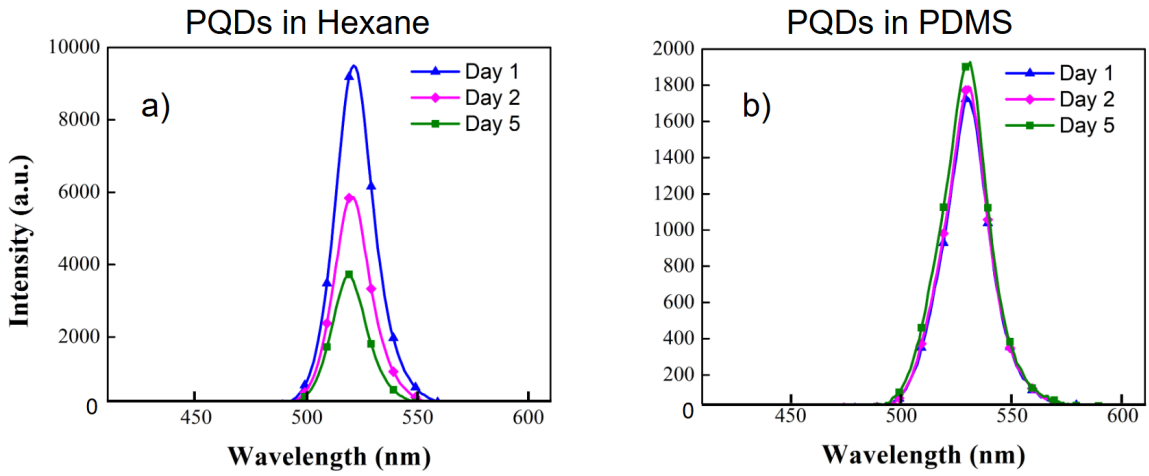

Figure 4.7. PL intensity graphs for PQDs in a) hexane (common solvent) b) embedded in PDMS for samples kept in the ambient conditions

Figure 4.7 shows that PDMS-encapsulated perovskite quantum dots maintain stable photoluminescence throughout a five-day test period whereas hexane-dispersed samples show quick degradation. The solid-state composite system demonstrates enhanced stability through multiple factors that result in decreased absolute emission intensity. These composites maintain stable emission properties which renders them especially suitable for specific optoelectronic uses in spite of their moderate intensity reduction. Passive display technologies achieve essential reliability by combining environmental stability with maintained color purity and solid-state

formats endure in downconversion applications (see Figure 4.8). Even though PDMS composite increases stability of PQDs in contrast to pure (not encapsulated) samples, it can't ensure long term stability due to containing metal catalysts as a curing agent [30]. Therefore there are other alternative polymers as poly(methyl hydrosiloxane) which is metal free and can be cured using different cross-linking mechanisms.

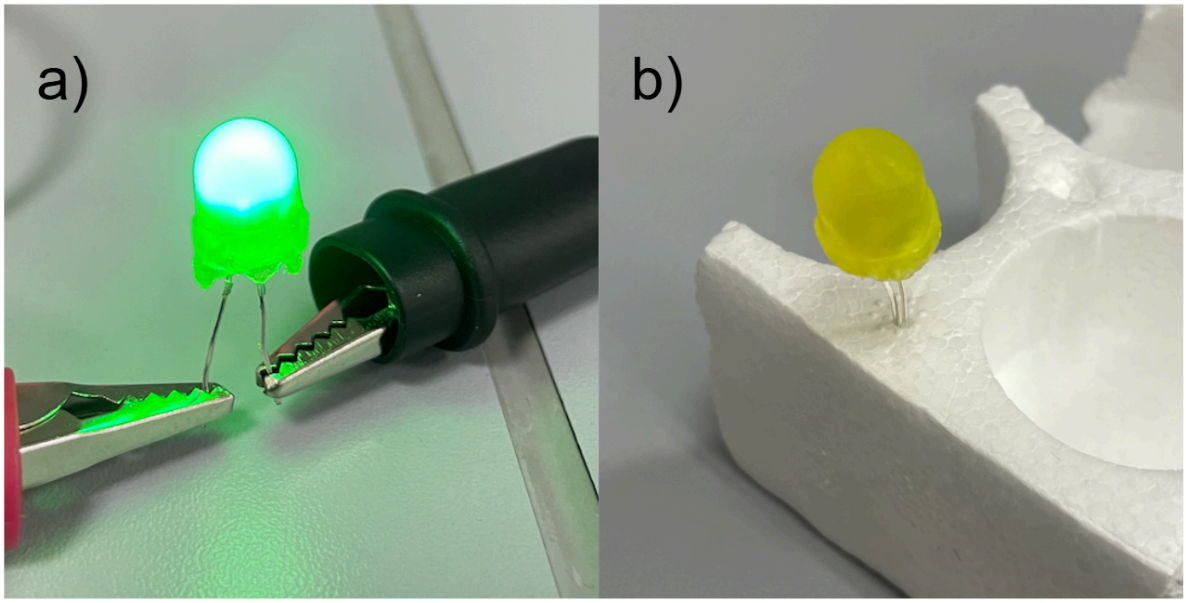

Figure 4.8. 395 nm UV LED covered with PQDs in PDMS compound a) voltage applied to terminal of LED, b) device in ambient

4.3 PQDs with PMHS

Poly(methyl hydrosiloxane) (PMHS) stands out as a desirable encapsulation material for perovskite quantum dots because of its non-toxic qualities and biomedical compatibility [30], however technical challenges hinder its application. The curing process for PMHS needs high thermal energy to activate polymerization because it sustains 80-120°C temperatures for multiple hours which approaches the stability boundary for various perovskite nanocrystal systems. The successful encapsulation of PQDs in PMHS shows environmental durability as they retain their

structural integrity during 24-hour water submersion tests. The inherent hydrophobic nature of the polymer combined with its dense cross-linked network produces an effective diffusion barrier that protects against moisture and oxygen. The PMHS system exhibits a critical problem because it intensely quenches PQD photoluminescence to the point where emission intensity becomes undetectable by conventional measurement devices. Despite the limitation on quantitative optical analysis capabilities the material demonstrates protective performance that indicates it could be useful in applications where environmental stability is more important than luminescent output such as some biomedical labeling or sensing applications.

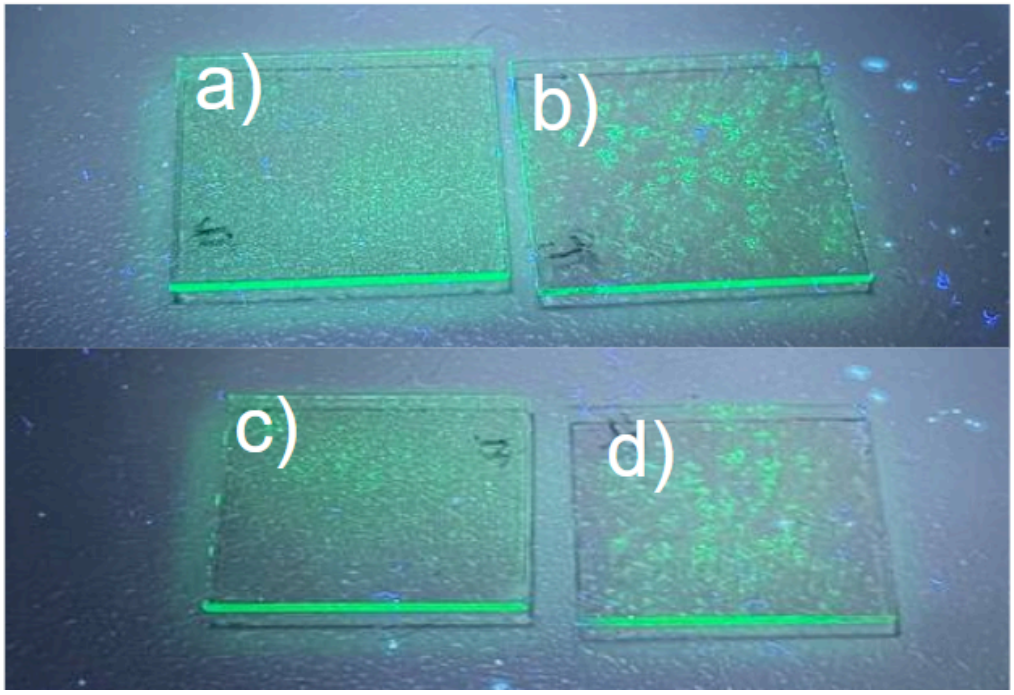

Figure 4.9. Before (a and b) and after (c and d) immersing PQDs@PMHS film in water. a and c) Premixed AIBN in PMHS before adding PQDs, b and d) AIBN, PMHS, and PQDs mixed and cured together

The brittle cured PMHS material's traditional limitation in device integration ends up enabling new processing techniques for perovskite quantum dot composites. The brittle mechanical properties of PMHS allow to pulverize PQD-embedded samples into fine powders using straightforward mechanical techniques to produce a versatile intermediate material. Through powderization the delicate bulk composite becomes a free-flowing particulate material which maintains the protective qualities of PMHS encapsulation. Once transformed into powder form quantum dot composites can be mixed into different polymer matrices using melt blending or solvent casting among other conventional processing methods. Multiple application opportunities exist through this processing method which allows the production of quantum dot masterbatches for extensive polymer manufacturing as well as the creation of luminescent inks and coatings and development of specialized composite materials. PMHS cannot be used directly in load-bearing or flexible applications due to its brittleness yet this same property becomes

beneficial when material processing is considered. Powder form conversion of protected quantum dots enables better compatibility with traditional manufacturing techniques and allows for broader application opportunities beyond the original PMHS matrix constraints.

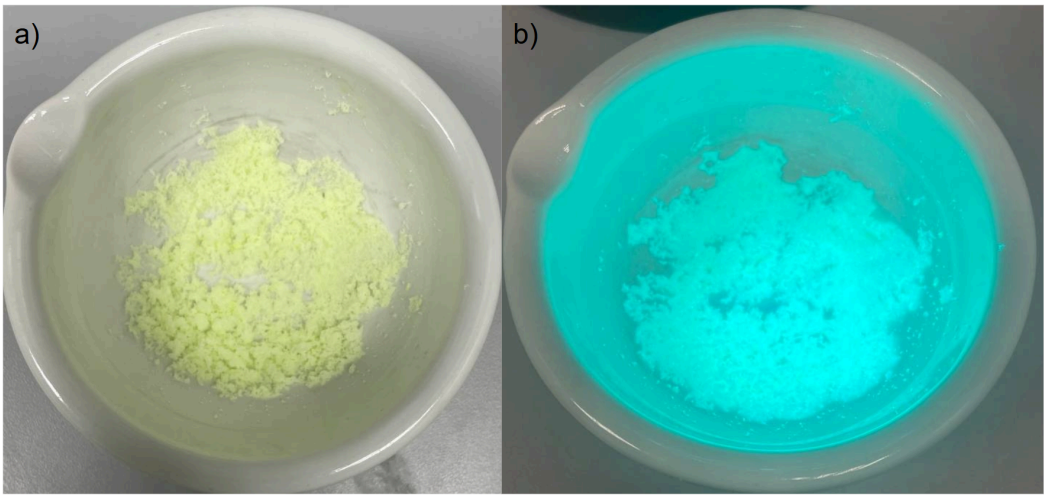

Figure 4.10. a) powdered PMHS with PQDs under room light, b) powdered PMHS with PQDs under UV illumination

4.5 Comparison of polymer matrices

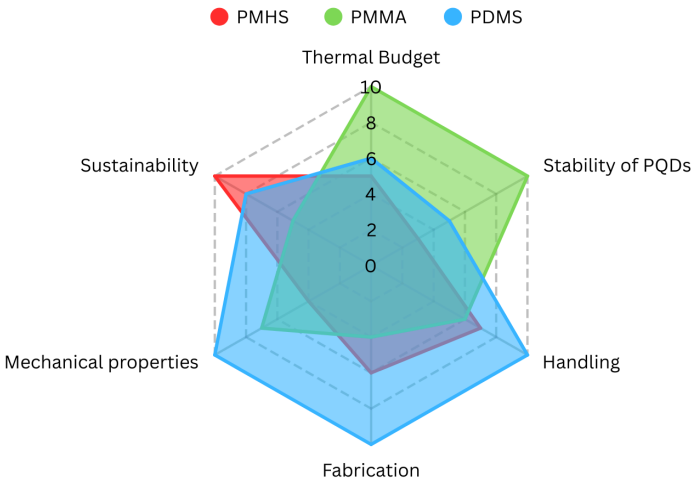

Figure 4.11. Comparing hexagon of polymer characteristics

The proper polymer matrix for PQD encapsulation needs to be selected through detailed analysis of processability capabilities along with stability features, thermal demands and environmental effects. PDMS, PMMA, and PMHS show unique properties that make them suitable for specific applications depending on their distinct characteristics shown in Figure 4.11.

PDMS stands out as the most adaptable choice because of its superior form factor flexibility. The liquid precursor state of PDMS allows it to be shaped into intricate forms demonstrated by the LED down-conversion cap in Figure 4.8. The material's ability to blend with hexane-suspended PQDs simplifies integration processes and the final cured elastomer exhibits strong mechanical durability even under stress. However, PDMS presents significant processing challenges. Room temperature curing can be performed but demands an unfeasible time span of 24-48 hours. The stability of embedded PQDs deteriorates when accelerated curing

is conducted at high temperatures such as 80°C for 2 hours which creates a severe limitation for thermal-sensitive uses.

PMMA provides exceptional environmental stability which preserves PQD photoluminescence for over 17 days under water without significant loss of light emission. The polymer enables composite creation at ambient temperatures through quick curing processes taking less than 30 minutes when kept below 50°C. However, PMMA processing introduces two significant complications. To achieve appropriate dispersion of PQDs within the PMMA matrix the necessary chlorobenzene solvent requires heating to about 69°C because it functions as an antisolvent. The growing porosity in PMMA films with increasing thickness from solvent evaporation limits their use to thin films to maintain uniform PQD distribution.

PMHS features distinctive benefits for certain applications despite its subpar mechanical performance. Prior to dissolution, the material experiences extreme brittleness along with PQD aggregation near AIBN particles. The PQD luminescence becomes notably degraded when thermal curing processes demand temperatures above 80°C sustained for 3 hours. PMHS stands out as the most eco-friendly choice because it eliminates the need for harmful solvents and metal catalysts in its curing process. This feature renders the material ideal for single-use or medical applications where ecological factors override mechanical needs.

Each polymer system shows specific advantages when analyzed comparatively. PDMS stands out for its use in applications requiring flexibility and shape adaptation like LED encapsulation and wearable sensors. PMMA shows outstanding performance in stable thin-film applications like displays and optical coatings. PMHS serves niche functions in low-stress situations where environmental considerations are crucial such as biodegradable sensors. Next-generation PQD encapsulation solutions would benefit from future studies that explore hybrid polymer systems which integrate the advantages of various materials while reducing their respective weaknesses.

Chapter 5 - Potential Applications

Integrating a Perovskite Nanocrystal layer into liquid crystal displays enables substantial improvements in the color purity of the images shown. The enhancement occurs through the inclusion of an extra layer containing PNCs which activates with blue light excitation [22]. The composite material exhibits a narrow emission spectrum in both green and red regions which increases color saturation and produces more vivid and precise visual displays [1]. PNC technology extends its potential to passive displays which find practical use in devices like emergency exit signs and low-power informational displays. The superior photoluminescence exhibited by perovskite quantum dots when activated by ultraviolet light delivers significant benefits for sophisticated sensor systems and particularly enhances the development of precise optical tactile sensing technologies. Under UV lighting PQDs generate narrow emission spectra with high quantum yields which produce intense pure fluorescence signals that significantly boost signal-to-noise ratios in detection systems[3]. The ability to track tiny deformations of marker arrays with high spatial and spectral resolution makes this characteristic indispensable for optical tactile sensing applications. PQDs produce sharp emission peaks that allow clear separation from background signals together with high brightness to enable detection of small positional changes when forces are applied. UV-excited fluorescence functions by generating electron-hole pairs within the PQD core which then quickly recombine radiatively. The controlled encapsulation of this process results in stable emission properties which remain unaffected by environmental changes and thus serve as perfect components for tactile sensing applications that demand sustained dependability. The adaptable photoluminescence properties of PQDs enable the creation of multiplexed detection methods which utilize distinct spectral signatures to represent different force magnitudes.

In tactile sensor applications, PQD markers are patterned into elastomeric substrates to enable the detection of mechanical deformation through changes in fluorescence distribution. Advanced image processing algorithms together with the optical excellence of PQDs provide enhanced force mapping capabilities for simultaneous detection of normal and shear forces at millinewton resolution. The development of PQD-enhanced tactile sensors now offers promising

applications for robotic manipulation and minimally invasive surgical systems which require precise force feedback [24].

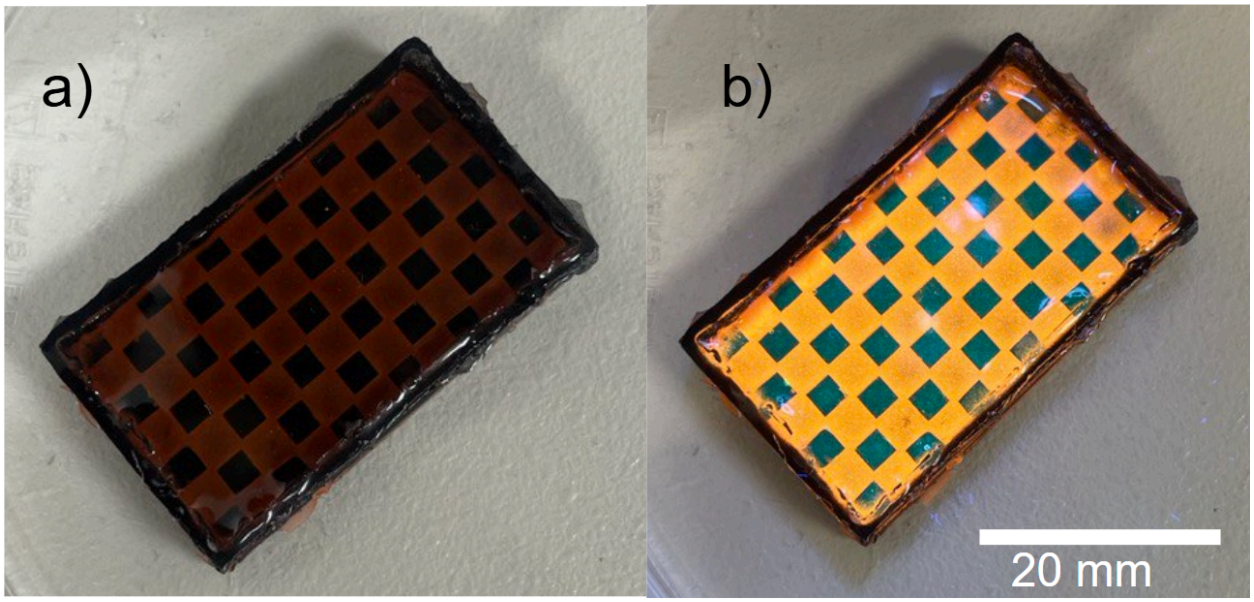

Figure 5.1. PQDs based tactile sensor (Type I) made from PDMS, a) sensor under room light, b) sensor under UV exposure

As illustrated in Figure 5.1 the optical tactile sensor that uses perovskite quantum dot (PQD) markers serves as an example of this new technology's potential benefits and difficulties. When UV light stimulates the system it performs at its peak using the PQDs' strong green light which sets up a vivid contrast with orange reference markers and this contrast allows for detailed monitoring of mechanical changes. The spectral differentiation between PQD markers and reference markers enables precise force mapping which surpasses the capabilities of traditional marker systems in ambient light conditions. Implementation remains impractical because material-related limitations continue to pose significant obstacles. The PDMS matrix delivers outstanding optical transparency and effortless manufacturing but requires a trade-off between mechanical strength and stability features. The sensor's sensitivity to minor force changes

becomes limited due to its moderate stiffness which has an elastic modulus ranging from 1 to 3 MPa especially for use cases that require high flexibility [31]. The trapped porosity within PDMS leads to environmental degradation of PQDs which results in observable luminescence decline after weeks of device operation posing significant barriers to industrial use. The performance limitations observed emerge from several factors that influence each other. Continuous UV exposure leads to photodegradation which diminishes marker brightness in PQDs with mechanical cycling speeding up this degradation by causing microstructural damage. The sensor's existing design fails to balance the initial precision benefits of rigid materials with the need for robust encapsulation to achieve long-term reliability. Enhancing sensor performance can be achieved through hybrid material systems that merge flexible substrates with superior barrier capabilities and advanced stability solutions such as core-shell quantum dots along with protective conformal coatings. These advancements will maintain the sensor's excellent initial performance while prolonging its useful life to satisfy real-world application standards.

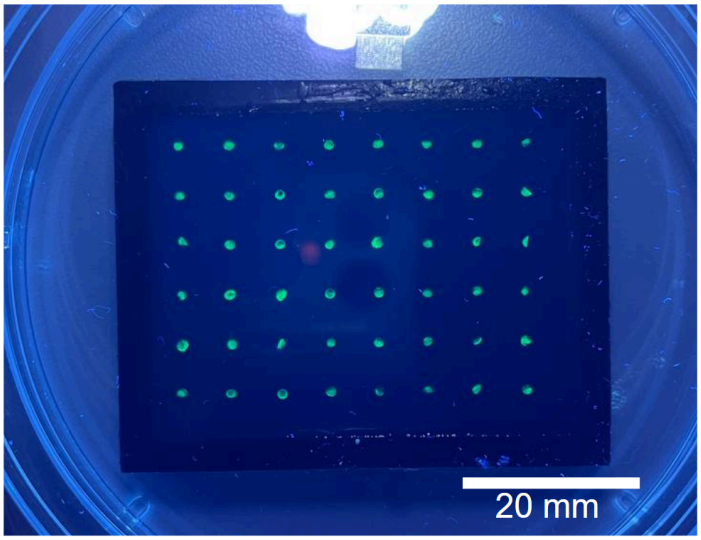

Figure 5.2. The tactile sensor (Type II) made by embedding PQDs in PMMA matrix exposed to UV light

Transition from PDMS to PMMA as the host matrix for PQD markers marks substantial progress in optical tactile sensor technology through extensive enhancements in performance and dependability. The improved barrier properties of PMMA protect luminescent quantum dots from environmental degradation factors and experimental evidence demonstrates that PQDs sustained in PMMA maintain their initial brightness even after 17 days submerged in water. The superior stability of PMMA stems from its natural low permeability to moisture and oxygen as well as its enhanced protection against UV light photodegradation [22]. The PMMA matrix allows for innovative sensor architectures that merge durable sensing layers with flexible substrates. The standard method involves PMMA dots embedded with PQD markers bonded to soft elastomer layers to produce a hybrid structure that delivers outstanding force sensitivity and durability. The compliant substrate layers generate strain concentration which boosts displacement in PMMA-embedded markers when force is applied.

PQD-based tactile sensing systems require a compact integrated optical system that merges UV excitation and visible light imaging. The best performance results when illumination and imaging components achieve coaxial alignment which is commonly set up with UV LEDs encircling the camera lens. Six 365 nm LEDs placed symmetrically around a camera can create enough irradiance to successfully activate markers. Advanced focus tracking algorithms correct sensor deformation when force is applied to maintain precise measurement throughout the entire operating range. Placement of lights near the camera requires specific shape of the UV LEDs. The best option to make it real is using surface mount LEDs on a printed circuit board. For such purposes schematic representation of circuit together with power unit created in EasyEDA software. As UV source 2W UVLEDs are used which are powered by voltage regulators designed to handle up to 5A current consumption.

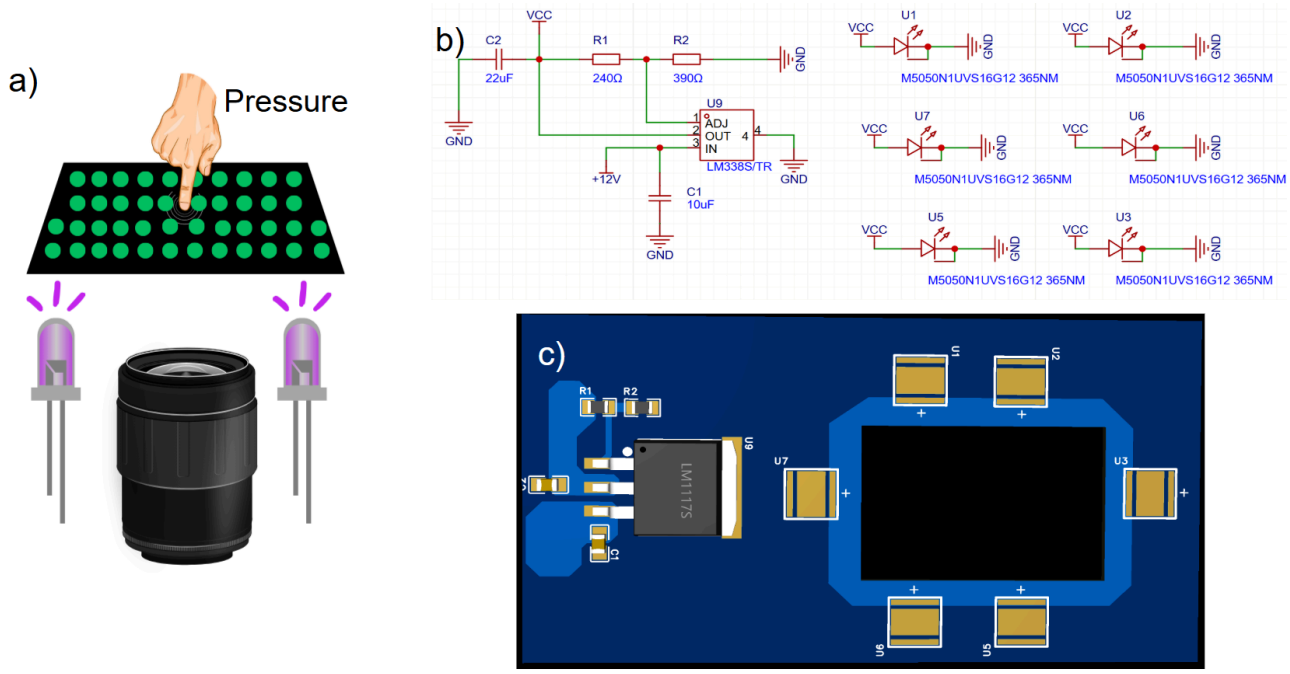

Figure 5.3. a) Schematic of electronic circuit driving LEDs, b) 3D top view of printed circuit board for LED installation

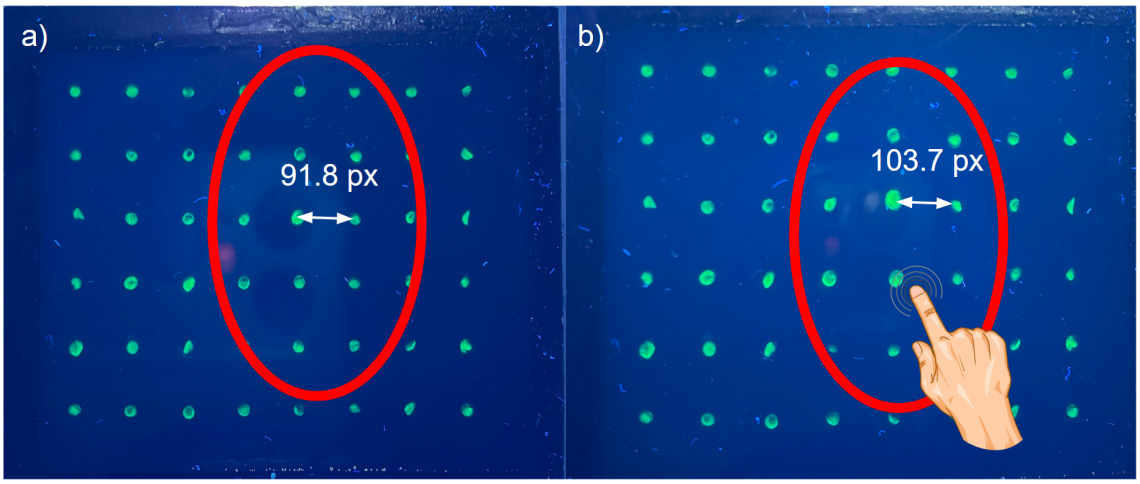

Figure 5.4. a) Optical tactile sensor without any acting force under UV illumination, b) Optical tactile sensor pushed by force under UV illumination

The tactile sensor's silicone layers exhibit compliant behavior that enables direct mechanical connection between force application and marker displacement which comparative images distinctly demonstrate. The separation between fluorescent markers on the sensor becomes measurable when pressure is applied which causes the distance to increase from 91.8 pixels at rest to 103.7 pixels during load application resulting in an 11.9 pixel displacement which functions as a reliable force measurement indicator. The correlation between displacement and force originates from basic elastomer mechanics since the low Young's modulus of soft silicone allows significant deformation with minimal force application. The silicone matrix demonstrates hyperelastic behavior which results in a repeatable nonlinear relationship between marker separation and applied force that sensor calibration can define. The execution of practical force measurement depends on implementing multiple computational processes. The initial calibration process sets up reference marker positions and identifies the sensor's distinct displacement-force response profile. Image processing algorithms may track marker movements in real time using centroid calculation or pattern matching methods while compensation routines handle the material's viscoelastic properties. After displacement measurements are obtained they can be transformed into force measurements by applying machine learning models developed from calibration datasets. This work does not include those measurements but it represents a potential area for future research enhancement.

Chapter 6 - Conclusion

This work explored different polymer matrix encapsulation methods for perovskite quantum dots (PQDs) to address their natural instability which restricts their use in optoelectronic devices. The study findings indicated that PMMA, PDMS, and PMHS present distinct benefits and limitations for which application-specific choices depend on how well they balance luminescent performance with mechanical flexibility and environmental durability and fabrication ease. PMMA-based composites showed superior durability in water-based environments due to core-shell siloxane functionalization. Extended water exposure did not affect the photoluminescence stability of QDs@SiO_2@PMMA systems because siloxane passivation effectively prevented environmental damage. The outstanding flexibility and processability of PDMS compensated for its slightly lower absolute PL intensity which makes it a perfect material to integrate PQDs into curved or stretchable devices like wearable sensors and LED covers. Flexible PQD-based tactile sensors demonstrated successful operation with visible marker displacement under mechanical force using PDMS which shows great promise for optical force sensing applications. Despite its severe luminescence quenching properties PMHS proved to be a promising encapsulant for biocompatible PQD powder formation which holds potential applications in microfluidics drug labeling and low-power photonics. Research comparing multiple polymer matrices showed that none of the materials function as the best solution under all circumstances. The combination of siloxane robustness with PDMS flexibility and PMMA water resistance can be achieved through hybrid and layered encapsulation approaches. Research in the future should investigate combined approaches with surface engineering methods such as ligand passivation and cutting-edge core-shell structures to maintain high PLQY and achieve extended operational durability. The findings from this research provide enhanced material design guidelines needed for dependable PQD applications within optoelectronic systems. The research bridges nanomaterials chemistry with polymer processing to provide important insights for creating robust and scalable functional composites used in high-performance sensors and light-emitting devices.

References

[1] L. Protesescu *et al.*, “Nanocrystals of Cesium Lead Halide Perovskites (CsPbX3, X = Cl, Br, and I): Novel Optoelectronic Materials Showing Bright Emission with Wide Color Gamut,” *Nano Letters*, vol. 15, no. 6, pp. 3692–3696, Feb. 2015, doi: 10.1021/nl5048779.

[2] T. C. Sum and N. Mathews, “Advancements in perovskite solar cells: photophysics behind the photovoltaics,” *Energy Environ. Sci.*, vol. 7, no. 8, pp. 2518–2534, 2014, doi: 10.1039/c4ee00673a.

[3] I. Dursun, C. Shen, B. S. Ooi, and O. M. Bakr, “Perovskite nanocrystals as color converters for record-breaking visible light communications,” *SPIE Newsroom*, Feb. 2017, doi: 10.1117/2.1201611.006756.

[4] W. Faschinger and J. Nürnberger, “Green II–VI light emitting diodes with long lifetime on InP substrate,” *Applied Physics Letters*, vol. 77, no. 2, pp. 187–189, Jul. 2000, doi: 10.1063/1.126919.

[5] J. Lin *et al.*, “Perovskite Quantum Dots Glasses Based Backlit Displays,” *ACS Energy Letters*, vol. 6, no. 2, pp. 519–528, Jan. 2021, doi: 10.1021/acsenergylett.0c02561.

[6] C. Wang *et al.*, “Controlled Synthesis of Composition Tunable Formamidinium Cesium Double Cation Lead Halide Perovskite Nanowires and Nanosheets with Improved Stability,” *Chemistry of Materials*, vol. 29, no. 5, pp. 2157–2166, Mar. 2017, doi: 10.1021/acs.chemmater.6b04848.

[7] T. A. Berhe *et al.*, “Organometal halide perovskite solar cells: degradation and stability,” *Energy & Environmental Science*, vol. 9, no. 2, pp. 323–356, 2016, doi: 10.1039/c5ee02733k.

[8] W. Cha, H.-J. Kim, S. Lee, and J. Kim, “Size-controllable and stable organometallic halide perovskite quantum dots/polymer films,” *Journal of Materials Chemistry C*, vol. 5, no. 27, pp. 6667–6671, 2017, doi: 10.1039/c7tc01562c.

[9] S. N. Raja *et al.*, “Encapsulation of Perovskite Nanocrystals into Macroscale Polymer Matrices: Enhanced Stability and Polarization,” *ACS Applied Materials & Interfaces*, vol. 8, no. 51, pp. 35523–35533, Dec. 2016, doi: 10.1021/acsami.6b09443.

[10] G. Li *et al.*, “Efficient Light-Emitting Diodes Based on Nanocrystalline Perovskite in a

Dielectric Polymer Matrix," *Nano Letters*, vol. 15, no. 4, pp. 2640–2644, Mar. 2015, doi: 10.1021/acs.nanolett.5b00235.

[11] L. Zhao *et al.*, "In Situ Preparation of Metal Halide Perovskite Nanocrystal Thin Films for Improved Light-Emitting Devices," *ACS Nano*, vol. 11, no. 4, pp. 3957–3964, Mar. 2017, doi: 10.1021/acsnano.7b00404.

[12] Y. Wei *et al.*, "Perovskite Quantum Dots: Enhancing the Stability of Perovskite Quantum Dots by Encapsulation in Crosslinked Polystyrene Beads via a Swelling–Shrinking Strategy toward Superior Water Resistance (Adv. Funct. Mater. 39/2017)," *Advanced Functional Materials*, vol. 27, no. 39, Oct. 2017, doi: 10.1002/adfm.201770230.

[13] E. Kang, G. S. Jeong, Y. Y. Choi, K. H. Lee, A. Khademhosseini, and S.-H. Lee, "Digitally tunable physicochemical coding of material composition and topography in continuous microfibres," *Nature Materials*, vol. 10, no. 11, pp. 877–883, Sep. 2011, doi: 10.1038/nmat3108.

[14] K. Ma, X.-Y. Du, Y.-W. Zhang, and S. Chen, "In situ fabrication of halide perovskite nanocrystals embedded in polymer composites via microfluidic spinning microreactors," *Journal of Materials Chemistry C*, vol. 5, no. 36, pp. 9398–9404, 2017, doi: 10.1039/c7tc02847d.

[15] M. Xia, J. Luo, C. Chen, H. Liu, and J. Tang, "Semiconductor Quantum Dots‐Embedded Inorganic Glasses: Fabrication, Luminescent Properties, and Potential Applications," *Advanced Optical Materials*, vol. 7, no. 21, Aug. 2019, doi: 10.1002/adom.201900851.

[16] X. Huang *et al.*, "Reversible 3D laser printing of perovskite quantum dots inside a transparent medium," *Nature Photonics*, vol. 14, no. 2, pp. 82–88, Nov. 2019, doi: 10.1038/s41566-019-0538-8.

[17] C. Liu, W.-T. Huang, and R.-S. Liu, "Stable glass-protected CsPbX3 (X = Cl, Br, and I) perovskite quantum dots and their applications in backlight LED," *Progress in Materials Science*, vol. 143, p. 101243, Jun. 2024, doi: 10.1016/j.pmatsci.2024.101243.

[18] S. Hou, Y. Guo, Y. Tang, and Q. Quan, "Synthesis and Stabilization of Colloidal Perovskite Nanocrystals by Multidentate Polymer Micelles," *ACS Applied Materials & Interfaces*, vol. 9, no. 22, pp. 18417–18422, May 2017, doi: 10.1021/acsami.7b03445.

[19] Q. Zhong *et al.*, "One-Pot Synthesis of Highly Stable CsPbBr3@SiO2 Core–Shell Nanoparticles," *ACS Nano*, vol. 12, no. 8, pp. 8579–8587, Jul. 2018, doi: 10.1021/acsnano.8b04209.

[20] B. Qiao *et al.*, "Water-resistant, monodispersed and stably luminescent

CsPbBr3/CsPb2Br5 core–shell-like structure lead halide perovskite nanocrystals," *Nanotechnology*, vol. 28, no. 44, p. 445602, Oct. 2017, doi: 10.1088/1361-6528/aa892e.

[21] Y. Huang *et al.*, "Enhancing the Stability of CH3NH3PbBr3 Nanoparticles Using Double Hydrophobic Shells of SiO2 and Poly(vinylidene fluoride)," *ACS Applied Materials & Interfaces*, vol. 11, no. 29, pp. 26384–26391, Jul. 2019, doi: 10.1021/acsami.9b07841.

[22] S. Yuan, Z.-K. Wang, M.-P. Zhuo, Q.-S. Tian, Y. Jin, and L.-S. Liao, "Self-Assembled High Quality CsPbBr3 Quantum Dot Films toward Highly Efficient Light-Emitting Diodes," *ACS Nano*, vol. 12, no. 9, pp. 9541–9548, Sep. 2018, doi: 10.1021/acsnano.8b05185.

[23] T. Li, W. Fu, C. Lei, and S. Hu, "Current status of anti-EGFR agents," in *Novel Sensitizing Agents for Therapeutic Anti-EGFR Antibodies*, Elsevier, 2023, pp. 1–12. Accessed: Apr. 14, 2025. [Online]. Available: https://doi.org/10.1016/b978-0-12-821584-5.00027-4

[24] J. Cheng *et al.*, "A Four-Capacitor Tactile Sensor Based on Bump Structure and Compensating Method to Reduce Inertial Interference for Robotic Tactile Sensing," *IEEE Sensors Journal*, vol. 23, no. 18, pp. 21670–21678, Sep. 2023, doi: 10.1109/jsen.2023.3291534.

[25] Y. Liu and M. Chen, "Applying text similarity algorithm to analyze the triangular citation behavior of scientists," *Applied Soft Computing*, vol. 107, p. 107362, Aug. 2021, doi: 10.1016/j.asoc.2021.107362.

[26] T. Li, W. Fu, C. Lei, and S. Hu, "Current status of anti-EGFR agents," in *Novel Sensitizing Agents for Therapeutic Anti-EGFR Antibodies*, Elsevier, 2023, pp. 1–12. Accessed: Apr. 14, 2025. [Online]. Available: https://doi.org/10.1016/b978-0-12-821584-5.00027-4

[27] K. Takashima, K. Ota, M. Yamamoto, M. Takenaka, S. Horie, and K. Ishida, "Development of catheter-type tactile sensor composed of polyvinylidene fluoride (PVDF) film," *ROBOMECH Journal*, vol. 6, no. 1, Dec. 2019, doi: 10.1186/s40648-019-0147-9.

[28] U. Kim, Y. B. Kim, D.-Y. Seok, J. So, and H. R. Choi, "A Surgical Palpation Probe With 6-Axis Force/Torque Sensing Capability for Minimally Invasive Surgery," *IEEE Transactions on Industrial Electronics*, vol. 65, no. 3, pp. 2755–2765, Mar. 2018, doi: 10.1109/tie.2017.2739681.

[29] Y. Li *et al.*, "Flexible PDMS/Al2O3 Nanolaminates for the Encapsulation of Blue OLEDs," *Advanced Materials Interfaces*, vol. 8, no. 20, Sep. 2021, doi: 10.1002/admi.202100872.

[30] M. Baeva *et al.*, "Enhancing the CsPbBr3 PeLEC properties via PDMS/PMHS double-layer polymer encapsulation and high relative humidity stress-aging," *Journal of Materials Chemistry C*, vol. 11, no. 43, pp. 15261–15275, 2023, doi: 10.1039/d3tc01370g.

[31] T. K. Kim, J. K. Kim, and O. C. Jeong, “Measurement of nonlinear mechanical properties of PDMS elastomer,” *Microelectronic Engineering*, vol. 88, no. 8, pp. 1982–1985, Aug. 2011, doi: 10.1016/j.mee.2010.12.108.